DIVERSITY OF A PHOSPHATE TRANSPORTER GENE AMONG SPECIES AND ISOLATES OF ARBUSCULAR MYCORRHIZAL FUNGI

ONE-SENTENCE SUMMARY

Phosphate transporter 1 gene sequences obtained from different AMF isolates represent a useful tool to highlight intraspecific diversity within the species *Funneliformis mosseae* and *Funneliformis coronatus*

Luca Giovannini[1a], Cristiana Sbrana[2a], Luciano Avio[1], Alessandra Turrini[1]

[1]Dipartimento di Scienze Agrarie Alimentari e Agro-ambientali, Pisa, Italy

[2]CNR, Istituto di Biologia e Biotecnologia Agraria, Pisa, Italy

[a]*These authors contributed equally to this work*

Keywords

Arbuscular mycorrhizal fungi; phosphate transporter genes; SSU-ITS-LSU region; intraspecific diversity; AMF molecular characterization; mycorrhizal symbiosis

Corresponding author: Alessandra Turrini, Dipartimento di Scienze Agrarie, Alimentari e Agroambientali, Via del Borghetto 80, 56124 Pisa, Italy. Phone +390502216646, e-mail alessandra.turrini@unipi.it

ABSTRACT

Arbuscular mycorrhizal fungi (AMF) are a key group of beneficial obligate biotrophs, establishing a mutualistic symbiosis with the roots of most land plants. The molecular markers generally used for their characterization are mainly based on informative regions of nuclear rDNA (SSU-ITS-LSU), although protein-encoding genes have also been proposed. Within functional genes, those encoding for phosphate transporters (PT) are particularly important in AMF, given their primary ability to take up Pi from soil, and to differentially affect plant phosphate nutrition. In this work, we investigated the genetic diversity of PT1 gene sequences and sequences of the taxonomically relevant SSU-ITS-LSU region in two isolates of the species *Funneliformis coronatus*, three isolates of the species *Funneliformis mosseae* and two species of the genus *Rhizoglomus*, originated from geographically distant areas and cultured *in vivo*. Our results showed that partial PT1 sequences not only successfully differentiated AMF genera and species likewise ribosomal gene sequences, but they also highlighted intraspecific diversity among *F. mosseae* and *F. coronatus* isolates. The study of functional genes related to the uptake of key mineral nutrients for the assessment of AMF diversity represents a key step in the selection of efficient isolates to be used as inocula in sustainable agriculture.

INTRODUCTION

Arbuscular mycorrhizal fungi (AMF) are a key functional group of beneficial soil microrganisms, that establish mutualistic symbioses with the roots of 80% of land plant taxa, including most major food and industrial crops, including cereals, pulses, potatoes, fruit trees, vegetables and medicinal herbs. AMF symbionts facilitate the uptake and transfer of mineral nutrients, such as phosphorus (P), nitrogen (N), sulfur (S), potassium (K), calcium (Ca), copper (Cu) and zinc (Zn), from the soil to the host plants, absorbed and translocated by the extraradical mycelium growing from mycorrhizal roots into the surrounding soil. In exchange, they obtain plant carbon, on which they depend as chemoheterotrophic organisms (Smith and Read 2008). AMF are fundamental components of sustainable agroecosystem processes and primary production, enhancing carbon

sequestration and soil aggregation, plant tolerance to biotic and abiotic stresses and increasing the content of healthy secondary metabolites, a distinctive characteristic of high-quality foods (Gianinazzi et al. 2010; Avio et al. 2018). Even though AMF are obligate biotrophic organisms, after establishing the symbiosis they produce asexual, multinucleate spores, whose phenotypic characteristics are utilized for their morphological identification and taxon attribution (Oehl et al. 2011; Redecker et al. 2013). AMF molecular identification is currently based on suitable molecular tools, which include informative regions of nuclear rDNA, spanning the end of the small subunit (SSU) gene, the highly polymorphic internal transcribed spacer region and the variable end of the large subunit (LSU), which are able to resolve even very closely related taxa (Krüger et al. 2009; Stockinger et al. 2010; Krüger et al. 2012). A number of candidate protein-encoding genes have been assessed for their ability to discriminate a few species of Glomeraceae (Ferrol et al. 2000; Helgason et al. 2003; Corradi et al. 2004; Msiska and Morton 2009; Sokolski et al. 2011). Within functional fungal genes, phosphate transporter (PT) genes are particularly important, given their primary ability to take up Pi from the soil solution, and to differentially affect plant phosphate nutrition (Ferrol et al. 2018). Accordingly, PT gene sequences have been utilized as a tool for species identification, in particular for differentiating morphologically identified species in the genus *Glomus*, many of which now affiliated to the genus *Rhizoglomus* (formerly known as *Rhizophagus*) (Sokolski et al. 2011; Savary et al. 2018). Such sequences were able to discriminate three *Rhizoglomus* species, but did not resolve the four distinct genetic groups identified by SNPs variations among isolates of *Rhizoglomus irregulare* (basionym *Glomus irregulare*; interim also known as *Rhizophagus irregularis*), cultured *in vitro* with Ri T-DNA transformed roots (Savary et al. 2018). Though, a high degree of sequence variation was observed within the different molecular marker regions, hampering the discrimination among co-specific isolates.

The main objective of this work was to assess whether sequences of the PT1 phosphate transporter, originally characterized in *Glomus versiforme* (Harrison and van Buuren 1995), could reveal genetic differences among isolates belonging to AMF species other than *Rhizoglomus*, and to

compare such differences with the genetic variation revealed by the sequences of the taxonomically relevant SSU-ITS-LSU region. To this aim, we investigated two isolates of the species *Funneliformis coronatus*, three of the species *Funneliformis mosseae* and two species of the genus *Rhizoglomus*, originated from geographically distant areas and maintained *in vivo*.

MATERIAL AND METHODS

Source and maintenance of the fungal material

The AMF isolates with different geographic origin used in this work belonged to the following species: *Funneliformis coronatus* (Giovann.) C. Walker & Schüßler (isolates IMA3 and BEG139), *Funneliformis mosseae* (T.H. Nicolson & Gerd.) C. Walker & A. Schüßler (isolates IMA1, IN101C, AZ225C), *Rhizoglomus irregulare* (Błaszk., Wubet, Renker & Buscot) Sieverd., G.A. Silva & Oehl, *Rhizoglomus venetianum* Oehl, Turrini & Giovann. (Table 1). Spores were obtained from pot-cultures maintained in the collection of the Microbiology Laboratories of the Department of Agriculture, Food and Environment, University of Pisa, Italy (International Microbial Archives, IMA), and produced in greenhouse, by growing *Medicago sativa* L. in 8.0 L plastic pots containing a mixture (1:1, by volume) of soil and calcined attapulgite clay (OILDRI, Chicago, IL). The soil was a sandy loam collected at the University farm, near S. Piero a Grado (Pisa). Chemical and physical characteristics of the soil used were as follows: $pH_{(H2O)}$, 8.0; clay, 15.3%; silt, 30.1%; sand 54.5%; organic matter, 2.2% (Walkley-Black); extractable P, 17.6 mg kg^{-1} (Olsen); extractable K, 149.6 mg kg^{-1}. The mixture was steam-sterilized (121°C for 25 min, on two consecutive days), to kill naturally occurring AMF. Each pot was inoculated with 2 L (25% of total pot volume) of a crude inoculum (mycorrhizal roots and soil containing spores and extraradical mycelium) of each isolate. After four months, spores and sporocarps were extracted from the soil of the pot cultures using the wet sieving and decanting technique, down to a mesh size of 50 μm (Gerdermann and Nicolson 1963). Spores retained on sieves, or extracted from sporocarps, were flushed into Petri

dishes and manually collected, with a capillary pipette under a dissecting microscope (Leica MS 5, Milan, Italy). Only intact, healthy spores were selected.

Phenotypic characterization

The presence of sporocarps was assessed for each isolate, together with sporocarp peridium colour and texture, and the number of spores per sporocarp. The colour and Melzer's reaction of endocarpic (excised from the sporocarps) and ectocarpic spores were also determined. Detailed microscopic examination of the spores was performed assessing spore colour and diameter, wall thickness, width and length of the subtending hypha, occurrence of the hyaline outer wall layer, after mounting in polyvinyl-alcohol lacto-glycerol (Omar, Bolland and Heather 1979) with or without the addition of Melzer's reagent. At least 50 individual spores were mounted on microscope slides and examined under a Polyvar light microscope equipped with Nomarski differential interference contact optics (Reichert-Young, Vienna, Austria).

Analyses of PT1 and SSU-ITS-LSU DNA regions

DNA extraction, amplification and sequencing

Spores obtained from *in vivo* cultures as described above were used for DNA extraction. 100 selected spores for each isolate were placed in an Eppendorf tube after sonication (120 s) in a B-1210 cleaner (Branson Ultrasonics, Soest, The Netherlands), washed three times in sterile distilled water (SDW) and surface sterilised with 2% Chloramine T supplemented with streptomycin (400µg/ml) for 20 min. After five rinses in SDW, spores were transferred into Eppendorf tubes, crushed with a glass pestle, and their DNA was extracted by using MasterPure yeast DNA purification KIT (Epicentre, Madison, USA) according to manufacturer's instructions.

A fragment of about 1500 bp, covering partial SSU, the whole ITS and the D1 and D2 variable regions of the LSU sequences of rDNA, was amplified using the nested protocol of Krüger et al. (2009). In the first PCR, a reaction mix of 25 µl was prepared using 0.625 U GoTaq Flexi

DNA Polymerase (Promega, Milan, Italy), 0.4 µM of each primer (SSUmAf1 and LSUmAr3, Krüger et al. 2009), 0.2 mM (each) dNTPs, 1.5 mM $MgCI_2$, and 1× manufacturer's reaction buffer. The thermal cycler was programmed as follows: a manual hot start at 95°C for 3 min, 35 cycles at 95°C for 30 s, 60°C for 1 min, 72°C for 2 min, and a final extension step at 72°C for 10 min. The nested PCR reactions were performed by diluting (1:100) the first PCR amplicons and using 2 µl of dilutions as template in a 50 µl reaction mix, containing 0.4 µM of the primer pair SSUmCf1-LSUmBr3 (Krüger et al. 2009), while Taq DNA polymerase, dNTPs, buffer, and $MgCl_2$ concentrations were the same as those described above. Amplification conditions were as follows: a manual hot start at 95°C for 3 min, 35 cycles at 95°C for 30 s, 63°C for 45 s, 72°C for 1.5 min, and a final extension step at 72°C for 10 min. PCR products (10 µl) were separated on 1% agarose gels containing Red Safe (0.05 µl ml^{-1}).

The primer pairs P6F (5'-AGTATTTGCTATGCAAGGATTT-3') and P6R (5'-GTCCACCAATGTCTTTTAGTTT-3'), or P7mF (5'-GTATTCGCGATGCAGGGATTC-3') and P7mR (5'-GGTCCACCAATGTCTTTTAGTTT-3') (Sokolski et al. 2011) were used to amplify PT1 region from the AMF isolates analysed. The 25 µl PCR mix contained 0.625 U GoTaq Flexi DNA Polymerase, 3 mM $MgCl_2$, 0.25 mM each dNTP, 1 µM each primer, 3 µl gDNA and 1× manufacturer's reaction buffer. Thermocycler conditions were as follows: 3 min at 95°C followed by 35 cycles at 95°C for 30s, 54°C for 45s and 72°C for 1min 30s, a final elongation step at 72°C for 10min.

Successfully amplified fragments of both SSU-ITS-LSU and PT1 regions obtained from each isolate were purified by Wizard SV Gel and PCR Clean-Up System according to the manufacturer's instructions (Promega), with a final elution volume of 20 µl, and purified products (2 µl) were quantified by a BioPhotometer (Eppendorf). Purified products were cloned into pGem®-T Easy vector according to the manufacturer's instructions (Promega). Putative positive clones were screened by standard SP6/T7 amplifications, followed by a nested PCR using the specific primer pairs for each amplicon and PCR conditions described above. Positive clones (3-4)

148 for each AMF isolate and amplified region were purified by Wizard® Plus SV Minipreps
149 (Promega). Recombinant plasmids were sequenced using SP6/T7 vector primers at GATC Biotech
150 (Köln, Germany) and sequences obtained were deposited in the European Nucleotide Archive
151 (http://www.ebi.ac.uk/ena/data/view/PRJEB35533).
152
153 *Sequence analyses*
154 Sequences were edited and aligned with those corresponding to the closest matches from the Basic
155 Local Alignment Search Tool (NCBI BLASTn) by using MUSCLE in MEGA X (Tamura et al.
156 2013).
157 Estimates of similarity between sequence pairs of either SSU-ITS-LSU or PT1 regions were
158 obtained from Clustal Omega Multiple Sequence Alignment tool
159 (https://www.ebi.ac.uk/Tools/msa/clustalo/) while divergence between the same sequence pairs
160 were computed using the Maximum Composite Likelihood model in MEGA X (Tamura et al. 2004;
161 Kumar et al. 2018). Data of similarity between sequences originated from the different AMF
162 isolates were used to draw matrix plots and those of divergence were used for Principal Coordinates
163 Analysis (PCoA), also known as Multidimensional scaling (MDS), using Past version 3.22. Using
164 the same software, a Mantel test (Mantel 1967, Mantel and Valand 1970) was computed
165 (permutation N = 9999) to test correlations between distance matrices obtained from SSU-ITS-LSU
166 and PT1 sequences.
167 On the basis of alignments with mRNA sequences showing high similarity, a 84 bp intron
168 (starting at position 722) was hypothesized to occur in PT1 DNA sequences of the different AMF
169 isolates analysed in this work. After removing the intron, putative partial protein sequences were
170 obtained using NCBI ORFfinder and verified with ExPASy translate tool. Partial putative protein
171 sequences were aligned using MEGAX with sequences of the crystal structure of a reference
172 eukaryotic phosphate transporter (PDB: 4J05_A), the phosphate transporter PHO84 from
173 *Saccharomyces cerevisiae* genome (NP_013583.1) and a phosphate transporter from *Rhizophagus*

irregularis DAOM 181602=DAOM 197198 genome (XP_025183371) to highlight the binding sites for phosphate.

Phylogenetic trees were inferred by Maximum Likelihood method based on the General Time Reversible model. The evolutionary rate differences among sites were computed in MEGAX using the model evolutionary rate differences among sites (5 categories (+G, parameter = 0.5181)). The confidence of branching was assessed using 1000 bootstrap resamplings. The generated phylogenetic tree was drawn in MEGAX and edited in Adobe Acrobat XI.

RESULTS AND DISCUSSION

Phenotypic characterization

The most remarkable difference among the three isolates belonging to the species *F. mosseae* was the absence of sporocarp production in the isolate IN101C, which was characterized by ectocarpic spores with significantly larger diameter, compared with AZ225C and IMA1 (Table 2), and also a larger hyphal attachment (51 ± 2 *vs*. 24 ±1 and 20 ±1 µm). Other differences among the isolates of *F. mosseae* were represented by the sporocarp texture, which was dense woolly in IMA1, while it showed a hard consistence in AZ225C, and by a large variation in the number of spores recorded in sporocarps of IMA1. However, IN101C, AZ225C and IMA1 isolates showed the typical spore wall features of *F. mosseae,* with an evanescent outer wall staining pink-red in Melzer's reagent, an inner laminated yellow wall with thickness ranging from 3.7 to 4.9 µm, and a funnel shaped subtending hypha. The spores of *F. coronatus* IMA3 and BEG139 were similar in colour, ranging from pale ochre to sienna to rust brown, but only IMA3 produced sporocarps (Table 2). As to *Rhizoglomus* isolates, their morphological characters were consistent with the species definition. Interestingly, the ability to form sporocarps, a morphological trait common to most isolates of *F. mosseae* and *F. coronatus* species (Giovannetti et al. 1991; Avio et al. 2009), was not shown by our isolates *F. mosseae* IN101C and *F. coronatus* BEG139, which formed only single spores. Actually,

sporocarp formation should be further investigated to assess whether this trait is stable at the isolate level and/or it is affected by environmental conditions.

Divergence and phylogenetic analyses of PT1 and SSU-ITS-LSU region sequences

Partial sequences of the Pi transporter gene obtained in this work ranged from 949 and 951 bp in length for *F. mosseae* and *F. coronatus* sequences, while for *R. venetianum* and *R. irregulare* they ranged from 969 and 971 bp. Variation of PT1 sequence lengths, which ranged between 800 and 1191 bp, was also reported in the same PT1 region for different isolates belonging to the species *R. irregulare* (Savary et al. 2018). The complete RiPT1 genomic sequence (accession KU219928) obtained from *R. irregulare* DAOM 197198 is 1742 bp (Walder et al. 2016) and encodes for a Pi transporter with large homology with the $Pi:H^+$ symporter ScPHO84 of *S. cerevisiae*, located in the plasma membrane (Wykoff and O'Shea 2001) and with the high-affinity (Km 18 μM) $Pi:H^+$ symporter of *Glomus versiforme* GvPT (Harrison and van Buuren 1991). PT1 orthologous genes, which were studied in *G. versiforme, R. irregulare, F. mosseae* and *Gigaspora margarita* were found to be expressed both in extraradical and intraradical mycelium, suggesting a main role in Pi uptake from the soil solution and also in Pi sensing and regulation of phosphate signaling at fungal/plant interface (Maldonado-Mendoza et al. 2001; Benedetto et al. 2005; Fiorilli et al. 2013; Xie et al. 2016).

PT1 sequence alignment revealed a high level of conserved regions, particularly among isolates of the same genus. Similarity among PT1 sequences obtained from isolates within the *Funneliformis* genus ranged between 92.9% (IN101C and IMA3) to 99.2% (IMA3 and AD1), while similarity between sequences from *R. irregulare* and *R. venetianum* was 94.7%. On the contrary, sequences from isolates belonging to the genus *Funneliformis* showed similarity lower than 75% compared with those of the two *Rhizoglomus* species (Fig. 1a). It was reported that PT1 sequence similarity among *R. irregulare* strains ranged from 99 to 100% (Savary et al. 2017), while 100% similarity was detected among *F. mosseae* strains different from those used in our study (Sokolski

et al. 2011). Interestingly, previously reported similarity between PT1 sequences of *F. mosseae* and *F. coronatus* was 94.5% and that between isolates belonging to the genera *Funneliformis* and *Rhizoglomus* was about 73% (Sokolski et al. 2011).

The first two coordinates of PCoA carried out on pairwise divergence of PT1 sequences obtained from AMF isolates accounted for 99% of variance, and the produced plot showed a clear separation between the AMF genera *Funneliformis* and *Rhizoglomus*, and between the species *F. coronatus* and *F. mosseae* (Fig. 1b). By contrast, low discrimination was obtained between the two *Rhizoglomus* species, while the *F. mosseae* isolate IN101C clustered in a different subgroup, as observed also for the two *F. coronatus* isolates.

Here PT1 phylogenetic analysis allowed the discrimination among closely related species and among different isolates of the same species, as IN101C formed a well defined cluster (99 boostrap value), within the species *F. mosseae* (Fig. 2) . Similarly, within *F. coronatus* clade the isolates IMA3 and BEG139 formed separate clusters (bootstrap value 90 and 65, respectively), confirming distance analysis data. In the *Rhizoglomus* group, *R. irregulare* IMA6 sequences grouped separately (bootstrap value 99), even from other *R. irregulare* sequences, while *R. venetianum* sequences were closer to *Oehlia diaphana* ones. Our PT1 phylogenetic analysis allowed the resolution of the four morphologically defined AMF species (*F. mosseae*, *F. coronatus*, *R. irregulare* and *R. venetianum*) and some co-specific isolates, confirming and expanding previous studies on the ability of PT1 gene sequences to discriminate among closely related AMF (Sokolski et al. 2011; Savary et al. 2018).

The analysis of putative partial PT1 protein sequences obtained from AMF isolates showed that similarity among *F. mosseae* isolates ranged from 93.1 to 98.6%, while that within the species *F. coronatus* was 99.3%, as for nucleotide sequences. Here, amino acid similarity between the species *R. irregulare* and *R. venetianum* was 87.2% and ranged from 84.8 to 90.5% between *F. mosseae* and *F. coronatus*. The latter species pair showed 94.5% similarity in PT1 sequences in a previous study (Sokolski et al. 2011). Compared with that reported in the quoted study (72.9-

73.1%), a lower similarity, ranging from 58.6 to 64.5%, was found between isolates belonging to the genera *Funneliformis* and *Rhizoglomus*. Phylogenetic analysis carried out with the deduced amino acid sequences of the PT1 genes showed a clustering at species and isolates level similar to that observed for nucleotide PT1 sequences (data not shown), suggesting that PT1 amino acid sequences could be also used as an AMF phylogenetic marker. In the complete sequence of *S. cerevisiae* PHO84 transporter, which is homologous to the AMF PT1 protein and is strongly induced under phosphate starvation conditions (Wykoff and O'Shea 2001), nine amino acids are known to represent binding sites for phosphate. Despite the differences detected in AMF PT1 nucleotide sequences, the alignment of putative partial protein of all isolates with sequences of *R. irregularis* PT1, with *S. cerevisiae* PHO84 and with the eukaryotic phosphate transporter 4J05_A showed four conserved phosphate-binding amino acids, the other being located in regions not amplified by our primer pairs. The conservation of amino acids whose residues are exposed into the phosphate-binding site of the transporter helix may be functional to the maintenance of both transport and signaling activities by the protein.

SSU-ITS-LSU sequences analyses showed an expected overall lower diversity, compared with PT1 sequences, among the AMF tested, though indicating similar trends in pairwise similarity among different genera and species and among co-specific isolates (Fig. 1c). Indeed, Mantel test, performed on divergence matrices obtained from the two genomic regions, showed a high and significant correlation among PT1 and SSU-ITS-LSU sequences of AMF isolates tested ($R = 0.99$, $p = 0.0001$).

Compared with that obtained from PT1 sequences, PCoA carried out on divergence data from SSU-ITS-LSU sequences produced a plot with similar clustering of data from the species *F. coronatus* and lower separation among *F. mosseae* isolates, while supporting a clear discrimination between the two *Rhizoglomus* species (Fig. 1d). The ribosomal region used in this study, including partial SSU rRNA gene, ITS region, and partial LSU rRNA gene, was reported to better discriminate AMF at the species- or isolate-level, compared with other rDNA fragments (Krüger et

277 al. 2009; Stockinger et al. 2010). Within this region, which was proposed as a barcode sequence for
278 fungi (Krüger et al. 2009), ITS2 represents the most variable sequence: indeed previous studies
279 reported mean intraspecific ITS2 divergence among *F. mosseae* isolates ranging between 1.2 and
280 4.8%, while the LSU and SSU rRNA genes showed values not exceeding 0.5% (Pellegrino et al.
281 2012).

282 As observed for PT1gene sequences, the phylogenetic analysis of SSU-ITS-LSU fragments
283 placed the four species within well supported clades (96-100 bootstrap value) (Fig. 3). Interestingly,
284 in our work AMF isolates of the different species were separated in defined clusters within the clade
285 of each species, so that they could be distinguished from each other. Blast analysis in MaarjAM
286 database showed that sequences of *F. mosseae* isolates IMA1, AZ225C and IN101 had a similarity
287 of 99.8%, 98.8% and 98.2%, respectively, with the isolate Att109-28 (BEG12, accession numbers
288 FR750028-30). *F. coronatus* isolate BEG 139 formed a separated cluster within *F. coronatus*
289 species, while IMA3 sequences were grouped with other *F. coronatus* sequences retrieved in
290 GenBank (isolate Att108-7, accession number FM87679897). Blast analysis in MaarjAM database
291 showed that sequences of *F. coronatus* isolate BEG139 and IMA3 had 97.4% and 99,2%
292 homology, respectively, with the *F. coronatus* sequence FM876798 (isolate Att108-7). Partial
293 sequences of ribosomal genes spanning the variable 3'end of the SSU gene, the highly polymorphic
294 internal transcribed spacer 2 (ITS2) and the variable 5' end of the LSU) were successfully used in a
295 previous work to discriminate the *F. mosseae* IMA1 and AZ225C isolates both between each other
296 and from native *F. mosseae* strains in the field (Pellegrino et al. 2012). Recently, the SSU-ITS-LSU
297 region was used to discriminate at subspecies level (Schlaeppi et al. 2016), even if such a region
298 generally provides resolution at species level (Krüger et al. 2012; Redecker et al. 2013). Our results
299 confirm the intrinsic variability occurring in the ribosomal region, which can indeed highlight also
300 small divergences among isolates.
301

302 **CONCLUSIONS**

In our work the analyses of partial PT1 sequences revealed intraspecific diversity among *F. mosseae* and *F. coronatus* isolates, in addition to the differentiation among AMF genera and species which was consistent with that obtained using ribosomal genes. Here, the genetic characterization was carried out on isolates maintained *in vivo*, as *in vitro* root-organ cultures, widely used so far, represents an artificial environment possibly leading to genetic and functional variations in cultured isolates, due to large nutrient availability, absence of hyphosphere/rhizosphere associated microorganisms and reduced host diversity (Kokkoris and Hart 2019).

The characterization of AMF isolates originating from different biomes and geographic areas showed the occurrence of different levels of phenotypic and genetic variability both among and within species (Opik et al. 2006; Davison et al. 2015; Savary et al. 2018). As geographically diverse AMF isolates may represent useful germplasm to assess the relationships between genetic diversity and functional traits, studies carried out using isolates maintained *in vivo*, such as those used in this work, may provide information relevant for evaluating host-symbiont interactions in natural and agricultural ecosystems. Actually, genetically different AMF isolates can cause large differences in Pi uptake and plant growth (Munkvold et al. 2004; Mensah et al. 2015; Rodriguez and Sanders 2015), possibly related to the expression and affinity of Pi transporter genes. In this view, the exploitation of AMF molecular and functional diversity represents a key step for the use of these beneficial fungi in sustainable agriculture.

FUNDING

This work was supported by a University of Pisa grant (Fondi di Ateneo).

Conflict of interest

The authors declare no conflict of interest.

REFERENCES

329 Avio L, Cristani C, Strani P *et al.* Genetic and phenotypic diversity of geographically different
330 isolates of *Glomus mosseae*. *Can J Microbiol* 2009;**55**:242-253.

331 Avio L, Turrini A, Giovannetti M *et al.* Designing the ideotype mycorrhizal symbionts for the
332 production of healthy food. *Front Plant Sci* 2018;**9**:1089.

333 Benedetto A, Magurno F, Bonfante P *et al.* Expression profiles of a phosphate transporter gene
334 (*GmosPT*) from the endomycorrhizal fungus *Glomus mosseae*. *Mycorrhiza* 2005;**15**:620-627.

335 Corradi N, Kuhn G, Sanders IR. Monophyly of -*tubulin* and *H-ATPase* gene variants in *Glomus*
336 *intraradices*: consequences for molecular evolutionary studies of AM fungal genes. *Fungal*
337 *Genet Biol* 2004;**41**:262–273.

338 Davison J, Moora M, Öpik M *et al.* Global assessment of arbuscular mycorrhizal fungus diversity
339 reveals very low endemism. *Science* 2015;**349**:970-973.

340 Ferrol N, Azcón-Aguilar C, Pérez-Tienda J. Arbuscular mycorrhizas as key players in sustainable
341 plant phosphorus acquisition: An overview on the mechanisms involved. *Plant Sci* 2019;
342 **280**:441-447.

343 Ferrol NJ, Barea M, Azcón-Alguilar C. The plasma membrane *H-ATPase* gene family in the
344 arbuscular mycorrhizal fungus *Glomus mosseae*. *Curr Genet* 2000;**37**:112-118.

345 Fiorilli V, Lanfranco L, Bonfante P. The expression of GintPT, the phosphate transporter of
346 *Rhizophagus irregularis*, depends on the symbiotic status and phosphate availability. *Planta*
347 2013;**237**:1267-1277.

348 Krüger M, Stockinger H, Krüger C *et al.* DNA-based species level detection of Glomeromycota:
349 one PCR primer set for all arbuscular mycorrhizal fungi. *New Phytol* 2009;**183**:212-223.

350 Krüger M, Krüger C, Walker C, *et al.* Phylogenetic reference data for systematics and
351 phylotaxonomy of arbuscular mycorrhizal fungi from phylum to species level. *New Phytol* 2012;
352 **193**:970-984.

353 Kumar S, Stecher G, Li M *et al.* MEGA X: Molecular Evolutionary Genetics Analysis across
354 computing platforms. *Mol Biol Evolut* 2018;**35**:1547-1549.

355 Gerdemann JW, Nicolson TH. Spores of mycorrhizal Endogone species extracted from soil by wet
356 sieving and decanting. *Trans Br Mycol Soc* 1963;**46**:235-246.

357 Gianinazzi S, Gollotte A, Binet MN, *et al.* Agroecology: the key role of arbuscular mycorrhizas in
358 ecosystem services. *Mycorrhiza* 2010;**20**:519-530.

359 Giovannetti M, Avio L, Salutini L. Morphological, cytochemical, and ontogenetic characteristics of
360 a new species of vesicular–arbuscular mycorrhizal fungus. *Can J Bot* 1991;**69**:161-167.

361 Harrison MJ, van Buuren ML. A phosphate transporter from the mycorrhizal fungus *Glomus*
362 *versiforme*. *Nature* 1995;**378**:626-629.

363 Kokkoris V, Hart MM. The role of *in vitro* cultivation on symbiotic trait and function variation in a
364 single species of arbuscular mycorrhizal fungus. *Fungal Biol* 2019;**123**:732-744.

365 Maldonado-Mendoza IE, Dewbre GR, Harrison MJ. A phosphate transporter gene from the
366 extraradical mycelium of an arbuscular mycorrhizal fungus *Glomus intraradices* is regulated in
367 response to phosphate in the environment. *Mol Plant-Microb Interact* 2001;**14**:1140-1148.

368 Mantel N. Ranking procedures for arbitrarily restricted observation. *Biometrics* 1967;**1**:65-78.

369 Mantel N, Valand RS. A technique of nonparametric multivariate analysis. *Biometrics* 1970;**1**:547-
370 558.

371 Mensah JA, Koch AM, Antunes PM *et al.* High functional diversity within species of arbuscular
372 mycorrhizal fungi is associated with differences in phosphate and nitrogen uptake and fungal
373 phosphate metabolism. *Mycorrhiza* 2015;**25**:533-546.

374 Msiska Z, Morton JB. Phylogenetic analysis of the Glomeromycota by partial -*tubulin* gene
375 sequences. *Mycorrhiza* 2009;**19**:247-254.

376 Munkvold L, Kjoller R, Vestberg M, *et al.* High functional diversity within species of arbuscular
377 mycorrhizal fungi. *New Phytol* 2004;**164**:357-364.

Nei M, Kumar S. *Molecular Evolution and Phylogenetics*. New York: Oxford University Press, 2000.

Oehl F, Sieverding E, Palenzuela J *et al.* Advances in glomeromycota taxonomy and classification. *IMA Fungus* 2011;**2**:191-199.

Omar M, Bolland L, Heather WA. A permanent mounting medium for fungi. *Bul Br Mycol Soc* 1979;**13**:31-32.

Öpik M, Moora M, Liira J, *et al.* Composition of root colonizing arbuscular mycorrhizal fungal communities in different ecosystems around the globe. *J Ecol* 2006;**94**:778-790.

Pellegrino E, Turrini A, Gamper HA *et al.* Establishment, persistence and effectiveness of arbuscular mycorrhizal fungal inoculants in the field revealed using molecular genetic tracing and measurement of yield components. *New Phytol* **2012**;194:810-822.

Redecker D, Schüßler A, Stockinger H *et al.* An evidence-based consensus for the classification of arbuscular mycorrhizal fungi (Glomeromycota). *Mycorrhiza* 2013;**23**:515-531.

Rodriguez A, Sanders IR. The role of community and population ecology in applying mycorrhizal fungi for improved food security. *ISME J* 2015;**9**:1053-1061.

Savary R, Masclaux FG, Wyss T *et al.* A population genomics approach shows widespread geographical distribution of cryptic genomic forms of the symbiotic fungus *Rhizophagus irregularis*. *ISME J* 2018;**12**:17-30.

Schlaeppi K, Bender SF, Mascher F *et al.* High-resolution community profiling of arbuscular mycorrhizal fungi. *New Phytol* 2016;**212**:780-791.

Smith SE, Read DJ. *Mycorrhizal symbiosis, 3rd edn*. London: Academic Press, 2008.

Sokolski S, Dalpé Y, Piché Y. Phosphate transporter genes as reliable gene markers for the identification and discrimination of arbuscular mycorrhizal fungi in the genus *Glomus*. *Appl Environ Microbiol* 2011;**77**:188-1891.

402 Stockinger H, Krüger M, Schüßler A. DNA barcoding of arbuscular mycorrhizal fungi. *New Phytol*
403 2010;**187**:461-474.

404 Tamura K, Nei M, Kumar S. Prospects for inferring very large phylogenies by using the neighbor-
405 joining method. *P Natl Acad Sci USA* 2004;**101**:11030-11035.

406 Turrini A, Saran M, Giovannetti M *et al. Rhizoglomus venetianum*, a new arbuscular mycorrhizal
407 fungal species from a heavy metal-contaminated site, downtown Venice in Italy. *Mycol Prog*
408 2018;**17**:1213-1224.

409 Xie X, Lin H, Peng X, *et al.* Arbuscular mycorrhizal symbiosis requires a phosphate transceptor in
410 the *Gigaspora margarita* fungal symbiont. *Mol Plant* 2016;**9**:1583-1608.

411 Walder F, Boller T, Wiemken A *et al.* Regulation of plants' phosphate uptake in common
412 mycorrhizal networks: Role of intraradical fungal phosphate transporters. *Plant Sign Behav*
413 2016;**11**:e1131372.

414 Wykoff DD, O'Shea EK. Phosphate transport and sensing in *Saccharomyces cerevisiae*. *Genetics*
415 2001;**159**:1491-9.

416

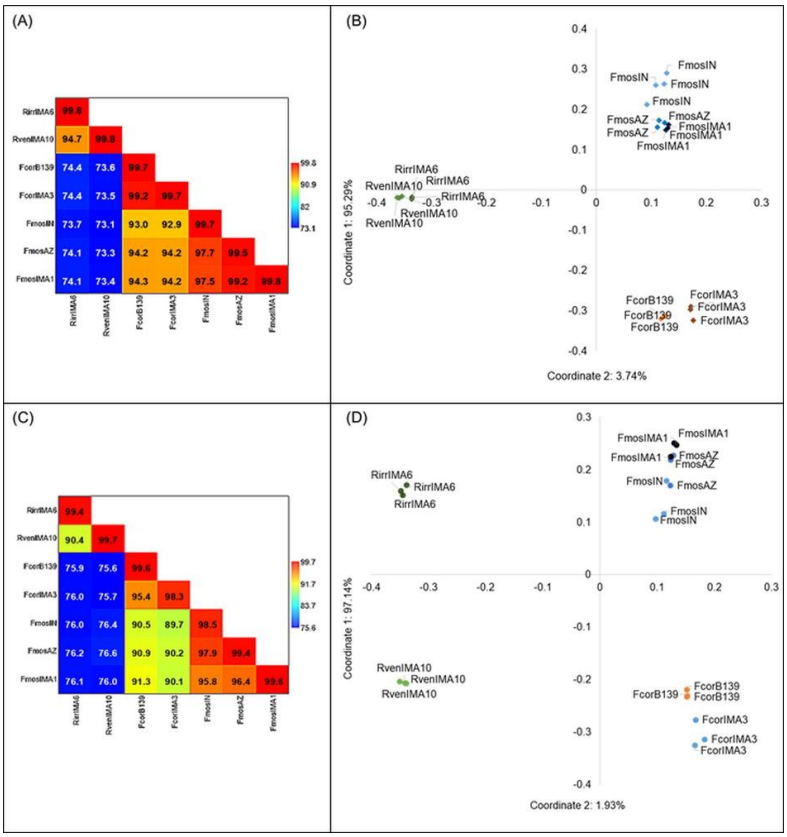

Figure 1. (A, C): cold-heat plots showing the averaged similarity among phosphate transporter 1 (A) or SSU-ITS-LSU (C) sequences obtained from the different arbuscular mycorrhizal isolates (computed from identity matrices generated for each pair of aligned sequences from Clustal Omega 2.1 multiple alignment tool). **(B, D)**: Principal coordinates analysis (PCoA) ordination based on phosphate transporter 1 (B) or SSU-ITS-LSU (D) sequences divergence among the arbuscular mycorrhizal isolates analyzed (carried out on the basis of divergence data computed in MEGA X, with a total of 1610 positions in the final dataset). Different colours depict different fungal isolates. The percentage of the variation explained by the plotted principal coordinates is reported on the axes.

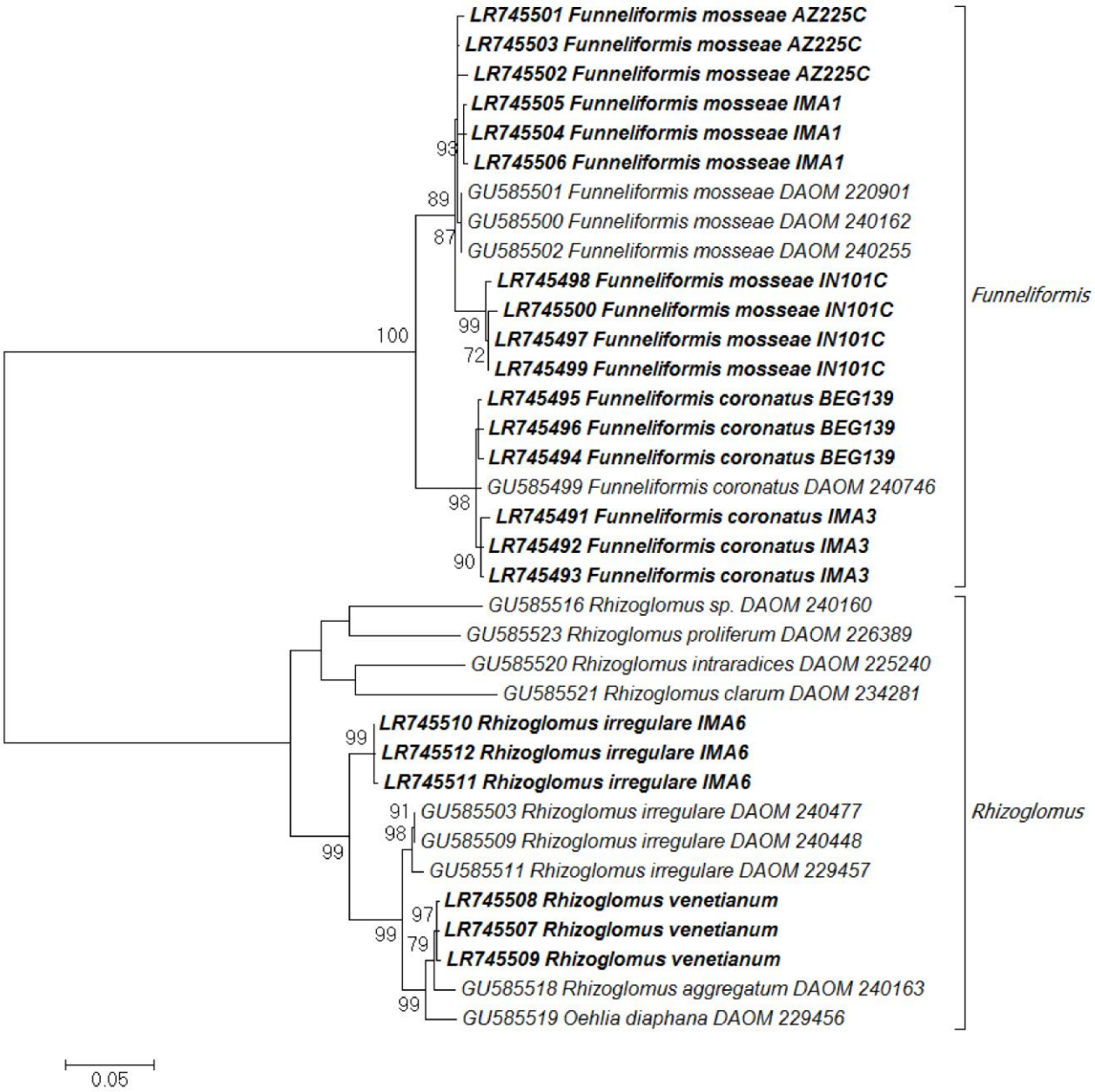

Figure 2. Maximum likelihood phylogenetic tree of glomeromycotan sequences obtained using the GTR + G model. The analysis is based on partial PT1 gene sequences (832 characters) and involved 35 nucleotide sequences. The ML bootstrap values are shown near the branches, when they exceed 70% (1000 replications). Sequences obtained in the present study are shown in bold, and their accession numbers are prefixed. Different genera are indicated in brackets.

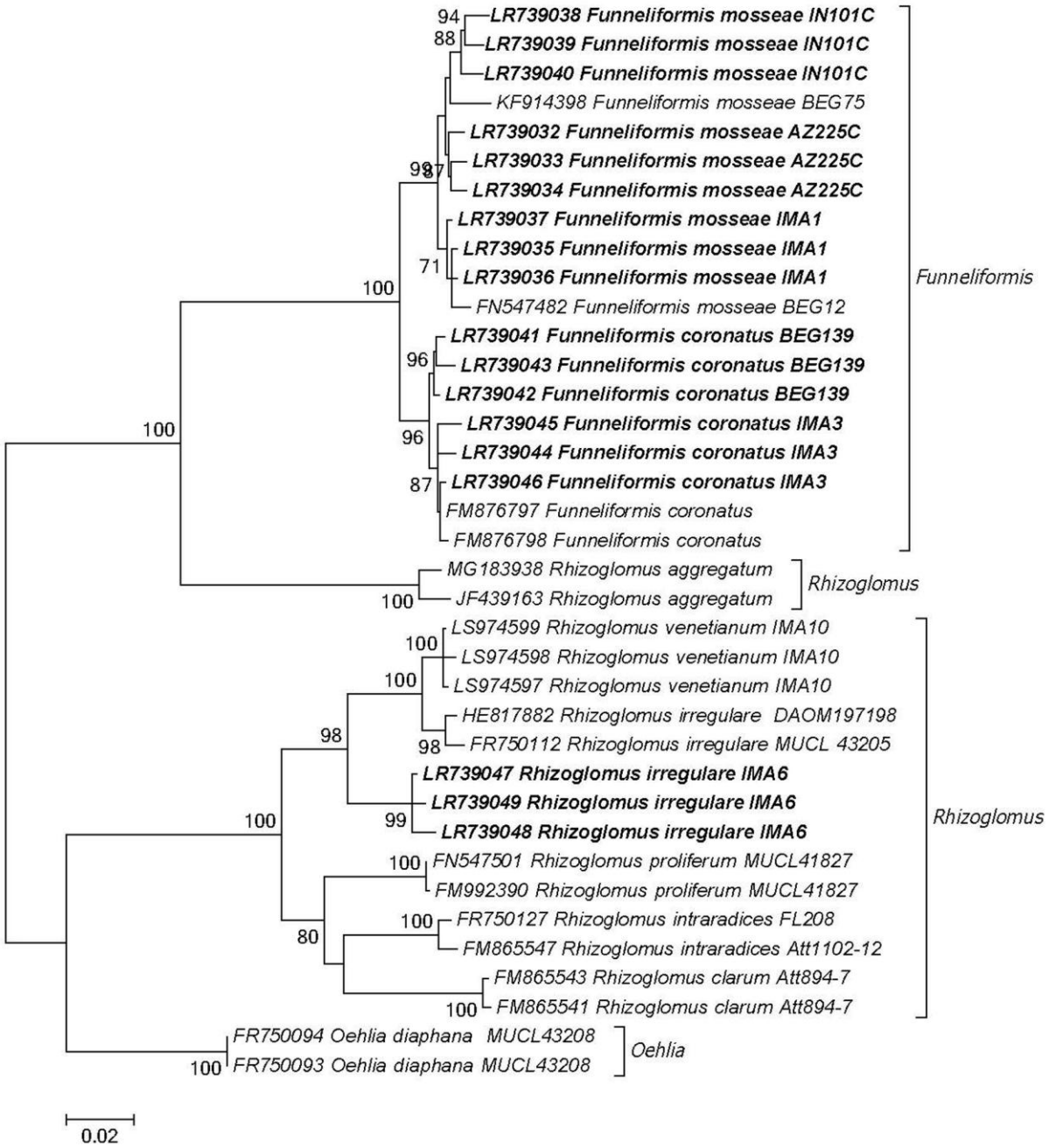

Figure 3. Maximum likelihood phylogenetic tree of glomeromycotan sequences obtained using the GTR + G model. The analysis is based on partial SSU, ITS, and partial LSU region of the nuclear rDNA sequences (1322 characters; SSUmCf3-LSUmBr1 fragment) and involved 37 nucleotide sequences. The ML bootstrap values are shown near the branches, when they exceed 70% (1000 replications). Sequences obtained in the present study are shown in bold, and their accession numbers are prefixed. Different genera are indicated in brackets.

444

445 **Table 1.** List of arbuscular mycorrhizal fungal isolates studied in the present work.

446

Fungal species	Isolate code	Geographic origin	Biome	Original inoculum supplier
Funneliformis coronatus	IMA3	Tuscany, Italy	Mediterranean sand dunes	IMA, Pisa, Italy
Funneliformis coronatus.	BEG139 (AD-1)	Abu-Dhabi, UAE	Subtropical desert	Dr. John Dodd, UK
Funneliformis mosseae	AZ225C	Arizona, USA	Subtropical desert	INVAM, Morgantown, WV, USA
Funneliformis mosseae	IMA1	Kent, UK	Unknown	Rothamsted Research, UK
Funneliformis mosseae	IN101C	Indiana, USA	Temperate grassland	INVAM, Morgantown, WV, USA
Rhizoglomus irregulare	IMA6	Burgundy, France	Temperate agriculture	INRA, Dijon, F
Rhizoglomus venetianum	IMA10	Venice, Italy	Contaminated site	IMA, Pisa, Italy

447

448 INVAM, International Culture Collection of (Vesicular) Arbuscular Mycorrhizal Fungi

449 IMA, International Microbial Archives

Corresponding author: Alessandra Turrini, Dipartimento di Scienze Agrarie, Alimentari e Agroambientali, Via del Borghetto 80, 56124 Pisa, Italy. Phone +390502216646, e-mail alessandra.turrini@unipi.it

450 **Table 2.** Phenotypic traits of arbuscular mycorrhizal fungal isolates studied in the present work

451

Isolate	Spore diameter	Sporocarp occurrence	Number of spores in sporocarps
Funneliformis coronatus IMA3	173-336	+	1-4
Funneliformis coronatus BEG139	140-180	-	-
Funneliformis mosseae AZ225C	148-320	+	1-5
Funneliformis mosseae IMA1	96-320	+	1-31
Funneliformis mosseae IN101C	160-336	-	-
Rhizoglomus irregulare IMA6	60-150	-	-
Rhizoglomus venetianum IMA10	72-145	+	>40[a]

452 [a] up to a few thousands of spores were reported.

453